

A key role for unusual spin dynamics in ferropnictides

I. I. Mazin and M. D. Johannes^{*}

The discovery of high- T_c ferropnictides introduced a new family of superconductors, and has already revealed a complicated and often contradictory picture of the structural and magnetic properties. An almost unprecedented sensitivity of the calculated magnetism and Fermi surface to structural details prevents correspondence to experiment. Experimental probes of the order parameter are in surprisingly strong disagreement, even considering the relative immaturity of the field. We outline various and seemingly contradictory evidence, both theoretical and experimental, and show it can be rectified by assuming a large-moment spin density wave, well defined but with magnetic twin and antiphase boundaries, dynamic on the experimental timescale. Under this assumption, calculations can accurately reproduce even very fine details of the structure, and a natural explanation for the temperature separation of structural and magnetic transitions is provided. Thus, our theory restores agreement between experiment and theory in crucial areas, making further cooperative progress possible on both fronts.

After two decades, a full understanding of the high- T_c cuprates has not been achieved, but in two major aspects there has been impressive progress¹. First, the symmetry of the superconducting symmetry is known: it is one-band $d_{x^2-y^2}$. Second, the parent compounds are understood as strongly correlated Mott insulators with local moments at the Cu sites linked by the superexchange mechanism. The essential physics is local and largely captured by the dynamical mean field theory (local by construction).

Neither of these things is known regarding the newly discovered ferropnictides². More importantly, it is known that the basic facts outlined above for cuprates do not apply to pnictides. The parent compounds are metallic and show weak magnetism rather than robust, localized moments. This magnetism is strongly affected by minor changes in the crystal structure and, in particular, by changes in the electronically inert rare-earth separator layer. This is in sharp contrast to the cuprates, which are completely insensitive to isoelectronic rare-earth substitutions. Andreev reflection^{3,4}, penetration-depth measurements⁵⁻⁷ and photoemission⁸⁻¹¹ all exclude the possibility of gap nodes, eliminating the standard d -wave superconductivity as we know it in cuprates.

One of the most mysterious differences between the cuprates and ferropnictides is the way in which standard density functional theory (DFT) band-structure calculations fail to describe them. In cuprates, DFT does not well describe the local Coulomb correlations that enhance the tendency toward local moment formation, and consequently barely magnetic or fully non-magnetic (NM) solutions result. Conversely, in the ferropnictides, calculations invariably converge to a spin density wave (SDW) state with magnetic moments significantly larger than experiment ($1.5-2 \mu_B$), whether in doped or in undoped materials¹²⁻¹⁴. Experimentally, antiferromagnetism is observed only at very low doping levels and is often very weak. The overestimation of magnetic strength compared to experiment is rare in DFT and definitively removes the ferropnictide family from the strongly correlated regime of the cuprates. Magnetic moments in both calculation and experiment seem to be very soft and change dramatically as a function of

seemingly minor details. Two calculational findings are particularly striking. First, enforcing a ferromagnetic (FM) ordering destroys magnetism nearly entirely^{12,15,16} (we were able to induce an FM moment comparable to the one calculated in the antiferromagnetic (AFM) ground state by applying in the calculations an external field of ~ 2 kT). Second, the total energies so obtained cannot be fitted to a Heisenberg model with first and second neighbours¹². This demonstrates that the magnetism is itinerant and requires coherence of at least several lattice parameters in order for a magnetic state to form.

We propose that these failures are due to an underlying ground state that is strongly magnetic, but with fluctuating domain boundaries that preclude its experimental detection. This simple assumption not only brings computational and experimental results into startlingly good agreement, but also provides a natural explanation for many experimental observations that otherwise seem incongruent. Below we summarize the current state of affairs with respect to what is known about the ferropnictides, experimentally and theoretically, pointing out where contradictions arise. We then show how a consistent picture can be formed by considering various features of our postulated magnetic state.

Experiment

It is well established^{17,18} that undoped LaFeAsO experiences a weak structural distortion at ~ 150 K, followed by formation of an SDW at ~ 140 K whose amplitude grows with cooling to $0.3-0.4 \mu_B$. The nearest-neighbour spins are aligned along one direction and anti-aligned along the other (see Fig. 1a,b). Such an ordering might, in principle, be explained by competition between AFM nearest- and next-nearest-neighbour couplings (if the former were about twice the latter). The surprisingly small observed ordered moment would then be attributed to frustration. However, this explanation cannot be right: magnetic frustration would lead to large static local moments near any crystallographic defect or impurity (see for instance LiV_2O_4 ; ref. 19) that would be detectable by muon spin resonance or Mössbauer experiments. Yet, both of these experiments find magnetic moments similar to, or even smaller

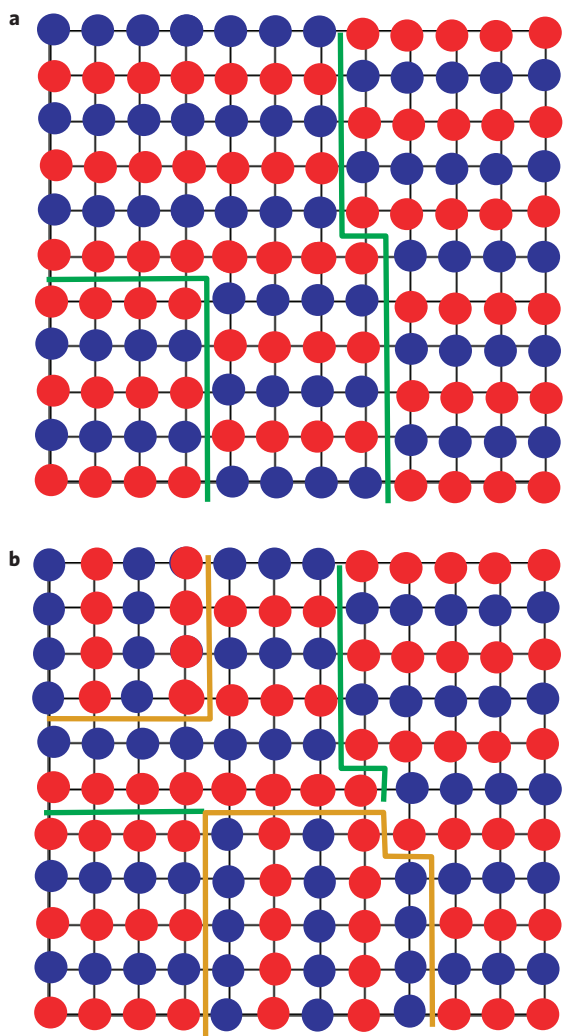


Figure 1 | Representative ferropnictide in-plane magnetic domains. **a**, Predominantly antiphase domains (pinned at $T < T_N$, dynamic at $T_N < T < T_S$). The x/y symmetry is broken. **b**, $T_S < T$ twin domains dominate, the global x/y symmetry is conserved. The green lines show antiphase domain walls and the brown lines the twin boundaries.

than, the ones measured with neutrons^{17,20,21}, even in bad and off-stoichiometric samples. In addition, as discussed below, such an explanation flatly contradicts first-principles calculations.

Isoelectronic manipulations within the (electrically charged, electronically inert) LaO layer affect the magnetism in an unexpectedly strong manner. In NdFeAsO the Fe moment remains $\sim 0.25 \mu_B$ until the Nd spins order at 2 K (refs 22,23). Most surprisingly, at this temperature the magnitude of the Fe moments jumps to $0.9 \mu_B$, more than three times as large^{22,23}! A Ce-substituted compound, like La, orders at about 140 K—but with a moment magnitude of $0.6 \mu_B$ (ref. 24). The Néel temperature T_N of Ce or Nd subsystems remains very low, of the order of 1–2 K, indicating an absence of noticeable magnetic coupling between the rare-earth and Fe moments. In fact, AFM ordering of Ce has been seen in superconducting samples²⁵, reinforcing the view that Ce f electrons are not coupled to Fe d states. This contrasts with the YBa₂Cu₃O₄ family, in which, except for Pr, no rare earths couple with the Cu d electrons, their ordering temperature remains low and they do not affect superconductivity. On the other hand, Pr does couple with the metallic states, orders at a temperature that is an order of magnitude higher and destroys superconductivity. Note that each rare-earth ion projects onto the centre of square Fe

plaquettes with equal numbers of up and down spins, so that within the Heisenberg model they do not couple with Fe moments at all. Finally, in BaFe₂As₂, which has no magnetic species besides Fe, the measured neutron moment is also close to $0.9 \mu_B$ (ref. 26) (although Mössbauer spectra suggest a moment half the size^{20,27}).

Contrary to initial expectation, the resistivity does not increase, or increases very little, on the onset of the SDW (which presumably gaps most of the Fermi surface), and then drops precipitously with further temperature lowering¹⁸. The in-plane to out-of-plane anisotropy does not change at all for the entire temperature range²⁸. This can be interpreted only as the rapid removal of some (isotropic) scattering channels at T_N that affects the overall carrier density only slightly²⁸. A sharp drop¹⁷ of the Seebeck coefficient right below the transition is even stronger evidence against a sharp drop in the carrier concentration, but is quite consistent with a rapid change of the transport relaxation time ratio.

The Seebeck coefficient for the doped compounds is anomalously large^{29,30}, in excess of $100 \mu V K^{-1}$, with a well-expressed maximum at ~ 100 K. This is typical of doped semiconductors rather than of sizeable-Fermi-surface metals, as these compounds are usually assumed to be.

Suppression of the static long-range magnetic order by doping has hardly any influence on the crystal structure, whereas suppression of the same by pressure is accompanied by a sharp drop in c/a ratio (and, correspondingly, the Fe–As bond length)³¹.

Experiments that directly or indirectly probe the superconducting gap and its symmetry have produced a variety of results. It is clear, nevertheless, that, although superconductivity arises in many members of the ferropnictide family as a function of doping, the doping level itself is actually irrelevant to the onset of pairing. The true controlling factor is the suppression of magnetism, which may be caused by doping, but can also be brought about by alternative means. It has been shown that when the long-range order is suppressed by pressure superconductivity appears, regardless of whether or not the compound is doped^{32,33}.

Theory

First-principles calculations predict a doping-independent metallic ground state with a large-amplitude SDW ($\mu = 1-2 \mu_B/Fe$) with the same ordering pattern as observed in experiment¹²⁻¹⁴. As opposed to most antiferromagnets, from Cr to NiO, the results of such calculations cannot be presented in terms of local moments interacting through pairwise exchange interaction. Unlike typical antiferromagnets, ferropnictides cannot be forced into a metastable FM state, though in a few cases an FM state with a very small moment (never comparable to the AFM solution) can be realized. If stabilization of the FM state is forced with an external field to compare it with AFM states, it seems that the corresponding energy differences cannot be mapped onto a two-nearest-neighbour Heisenberg Hamiltonian. Finally, exchange parameters calculated as the second derivative of the total energy with respect to the spin misalignment angle strongly depend (even in sign!) on the underlying ordering pattern^{13,34}. For instance, for the actual AFM stripe ordering, the calculated exchange constant between anti-aligned neighbours is 550 K and that for aligned neighbours is -80 K (ref. 13). Obviously, for a checkerboard ordering (all nearest neighbours anti-aligned), the two constants must be equal. Finally, the calculated NM state is stable against small perturbations¹³ (that is, the spin susceptibility does not diverge at the wavevector required for the observed SDW); nonetheless, a finite amplitude SDW is substantially more stable than the NM state. The origin of magnetism is similar to that in metal iron: it is driven by competition between the intra-atomic Hund's rule coupling, I , and the loss of one-electron energy associated with exchange splitting. A small NM DOS, N , compared to metal iron makes LaFeO_xF_{1-x} stable, or barely unstable against an FM instability ($IN \sim 1$), but

Table 1 | Calculated and experimental As positions and Fe moments.

	Exp.	GGA-NM		GGA-AF		GGA
	z_{As}	z_{As}	Error (Å)	z_{As}	Error (Å)	μ (calc.)
LaFeAsO	0.6513	0.6375	0.12	0.6478	0.03	2.06 μ_{B}/Fe
BaFe ₂ As ₂	0.3545	0.3448	0.13	0.3520	0.03	1.97 μ_{B}/Fe
LaFePO	0.6339	0.6225	0.05	0.6254	0.03	0.60 μ_{B}/Fe

These and other computational results in this paper have been obtained using the full-potential LAPW method, in the WIEN2k implementation, as described in ref. 13.

formation of the SDW opens a pseudogap at the Fermi level and offsets the loss of one-electron energy due to exchange splitting. Only by opening a pseudogap can iron fully realize its propensity toward strong magnetization. Therefore, this pattern is by far the most stable (a detailed analysis of the energetics of magnetism formation in ferropnictides will be published elsewhere).

Structural optimization without accounting for magnetism leads to Fe–As or Fe–P bonds that are much shorter than those observed experimentally (by up to 0.15 Å). On the other hand, allowing for full spin polarization leads to pnictogen positions that are very close to the experiment (errors less than 0.03 Å), but yield a very large magnetic moment ($\mu \sim 1\text{--}2 \mu_{\text{B}}/\text{Fe}$) not seen in experiment. This holds for all three major ferropnictides: LaFeAsO, BaFe₂As₂ and LaFePO. The last of these is fully NM experimentally and the calculated ground-state moment is much smaller (0.6 μ_{B}) in comparison with the other two types. Correspondingly, the error in the calculated Fe–P bond length in the NM case is also much smaller (0.05 Å) than in the other two families (Table 1). It seems that the discrepancy between the calculated Fe–pnictogen bond length and the experiment is directly proportional to the calculated ground-state magnetic moment! Furthermore, calculations in which Fe carries a reasonably large moment lead to correctly reproduced pnictogen positions regardless of the particular ordering pattern chosen. We have verified that optimizing the As and La positions within the checkerboard AFM structure, which is entirely different from the observed SDW, yields nearly the same coordinates as using the actual SDW ground-state magnetic pattern, as long as the Fe moment is large. Probably the most striking indication of a drastic effect of magnetism on crystal structure is the fact that when magnetism in CaFe₂As₂ is removed by pressure (first-principles calculations^{31,35} suggest that not only static long-range order, but also the local moments themselves, are suppressed by pressure), the crystal structure collapses from that corresponding to the fully magnetic generalized gradient approximation (GGA) to that corresponding to NM calculations³⁵. The final piece of evidence comes from the observation³⁶ that NM first-principles calculations provide an excellent description of the experimental phonon spectra, but only after the calculated Fe–As force constant has been reduced by 30%. We have verified that allowing for full AFM reduces this force constant by 25–35%, depending on the computational details.

The structural distortion observed in experiment cannot be reproduced using NM calculations. Establishing the AFM stripe phase again resolves the problem and, as observed experimentally^{37,38} and computationally^{14,38}, we obtain the relative contraction of the Fe–Fe distance between parallel spin neighbours compared with antiparallel neighbours, using a full structural relaxation as described in ref. 12. In contrast to the Fe–As distance, however, obtaining the structural distortion requires that the correct SDW pattern be applied. In the AFM checkerboard pattern, just as in NM calculations, Fe–Fe neighbours along both directions are equidistant and the ground-state structure remains undistorted. This suggests that the structural transition is driven by the AFM stripe magnetism, despite the fact that the magnetic

transition occurs at a lower temperature than the structural one. It is worth noting that, although it is not necessarily the strongest superexchange interaction, the one due to direct Fe–Fe overlap is most sensitive to the Fe–Fe distance. In other words, if the magnetic ordering were being driven by superexchange, the AFM bonds would contract, in contrast to the observed and calculated expansion.

In view of the above-mentioned temperature-independent transport anisotropy, we have calculated the squared plasma frequency (which corresponds to the resistivity anisotropy in the isotropic-scattering approximation), and found that the anisotropy is about five times larger in the stripe AFM phase than in the NM phase, in contradiction with the experimental observation that the onset of the SDW does not change the anisotropy. The calculated value of the squared plasma frequency (that is, effective number of carriers) in the AFM phase is one order of magnitude smaller than in the NM phase, whereas in the experiment the resistivity of the high-temperature phase extrapolates at zero temperature to a number at least twice as large as the actual low-temperature resistivity in the AFM phase.

In the energy-independent relaxation-time approximation, we calculated the Seebeck coefficient (in the energy-independent scattering-time approximation and using the calculated dependence of the plasma frequency on the Fermi energy) in the NM phase to be just a few $\mu\text{V K}^{-1}$, and with the wrong sign compared with experiment. Yet again, allowing for full spin polarization (1.8 μ_{B}/Fe) in the AFM phase brings it within a reasonable range of the experimental value of $\sim -100 \mu\text{V K}^{-1}$.

A dynamic spin-density-wave system

It is possible to reconcile almost everything known about these ferropnictides and their properties, as laid out above, by assuming that the underlying system truly is magnetic. First, we assume that the mean-field ground state of an ideal system is stripe AFM with a large moment that is close to the DFT-calculated one, but which is likely to be reduced to $\sim 1 \mu_{\text{B}}$ by conventional zero-point fluctuations. The magnetic energy associated with this moment is responsible for expanding the Fe–As bond and driving the orthorhombic distortion, and thus computational and experimental structures are in excellent agreement. However, given the small energy difference between the AFM stripe magnetic structure and other AFM patterns^{12,39}, a large number of antiphase boundaries will form, even at very low temperatures (Fig. 1a). Moreover, as the interlayer magnetic interactions are extremely small (our calculations put an upper bound of a few K for the interlayer exchange), the concentration of stacking faults along the z direction should be exceedingly large. Without a more detailed theory, it is difficult to quantify the dynamics of these defects (antiphase boundaries and stacking faults), but, as there is no clear mechanism for pinning, they probably do not fully freeze in even at relatively low temperatures. The interlayer magnetic coherence in particular is probably very fragile, and, correspondingly, a true long-range order would occur only in a small fraction of the sample (or in none at all) and would be suppressible by doping.

Furthermore, fluctuations that correspond to the SDW wavevector along the two directions, that is $Q_x = (\pi, 0)$ and $Q_y = (0, \pi)$, will suppress long-range order in two dimensions, but will be strongly reduced by any three-dimensional interaction. Such fluctuations probably play a large part in the unusual sensitivity of the magnetic transition to the rare-earth layer that effectively controls the three-dimensionality of the compound. In other words, most of the Fe ions will be part of an SDW domain at any given moment of time, but will flip their spin every time a domain wall passes through that site. On the timescale of muon spin resonance or Mössbauer spectroscopy (10^{-8} s or slower) these sites will be observed to have substantially reduced moments or seem completely NM.

According to this scenario, below T_N (where the SDW order becomes detectable) the antiphase boundaries are pinned by the establishment of three-dimensional coherency. For $T_N < T < T_s$ (where T_s is the structural transition temperature), there is no long-range magnetic order owing to the now dynamic antiphase boundaries, but the x/y symmetry is violated: all magnetic domains have the same orientation (Fig. 1a). At T_s , the system moves from a state dominated by antiphase boundaries where little twinning exists to a state in which the main defects are twin domain walls (Fig. 1b). According to recent data¹⁷, twinning is incomplete all the way up to $T \sim 200$ K, with an imbalance between x - and y -oriented AFM domains remaining at all lower temperatures. At higher temperatures, the concentration of the two domain orientations is the same, and the global symmetry is tetragonal. Twinning rapidly disappears on cooling below T_s and is nearly (though still incompletely, according to ref. 17) absent below T_N , at which temperature the three-dimensional coherency first sets in. As the twin and antiphase boundaries are electronically different, they scatter electrons differently so that both transitions are expected to be observable in transport properties. Indeed, the differential resistivity, $d\rho(T)/dT$, shows a sharp change of slope²¹ at T_s and a peak at T_N . The rapid drop in resistivity below T_N in single crystals is thus associated with freezing of the domain walls. Note that in this model neither the band structure nor the carrier concentration changes drastically at T_s or T_N —the relaxation rate does. This explains the surprising invariance of the resistivity anisotropy over the entire temperature range. Note that the picture visualized by Fig. 1a,b is useful, but probably oversimplified. More rigorously, above T_s SDW fluctuations with $q = Q_x$ and Q_y have the same weight, whereas below T_s fluctuations with one particular wavevector dominate, thus breaking the x/y symmetry.

As the carrier scattering is magnetic in origin, interesting magnetoelastic effects can be expected. A large magnetoresistance has indeed been observed in BaFe_2As_2 (ref. 28) at $T \lesssim 100$ K. The small carrier concentration in the magnetic phase also helps to explain the large thermopower. Finally, the mysterious sensitivity of the magnetic ordering to the character of the inert space-filling layer (LaO, CeO, SmO, Ba, Eu etc) finds a natural explanation: the establishment of long-range magnetic order is a three-dimensional phenomenon. Although most of the physical properties of the system are defined by the formation of AFM domains in individual planes, a detectable long-range ordering and a transition from the slow dynamics of domain walls (zero net magnetization on any given site over a long period of time) to their freezing requires three-dimensional coherency. This last process is sensitive to the properties of the filling layer, such as the presence of magnetic moments, despite the near-complete lack of magnetic interaction between the rare earth and iron.

It is also tempting to associate some of the gaps observed in PCAR (refs 3,4) and ARPES (refs 8–10) with a dynamic SDW (pseudo)gap. In fact, the authors of several experimental reports already favour such an interpretation^{3,11}. At the present stage, the dynamic-magnetic-domain scenario remains a hypothesis, albeit an attractive one that unites theory, experiment and previously

irreconcilable observations. The goal of this paper is to attract the attention of experimentalists and theorists to this possibility. Currently, no other model consistently explains the entire body of experimental and computational evidence. It remains to be seen how unusual, topological excitations such as antiphase and twin domain boundaries may affect and/or possibly cause the high-temperature superconductivity in ferropnictides.

After the initial submission of this manuscript, spectroscopic measurements that showed large moments on Fe in formally NM samples⁴¹, or even two transition temperatures, interpreted as local magnetic and structural transitions⁴⁰, were reported. Both transitions survived well into the superconducting region as a function of electron doping. This fits extremely well with the picture presented in our work.

Received 29 August 2008; accepted 19 November 2008;
published online 21 December 2008

References

- Lee, P. A., Nagaosa, N. & Wen, X.-G. Doping a Mott insulator: Physics of high-temperature superconductivity. *Rev. Mod. Phys.* **78**, 17–85 (2006).
- Kamihara, Y., Watanabe, T., Hirano, M. & Hosono, H. Iron-based layered superconductor $\text{La}[\text{O}_{1-x}\text{F}_x]\text{FeAs}$ ($x = 0.05\text{--}0.12$) with $T_c = 26$ K. *J. Am. Chem. Soc.* **130**, 3296–3297 (2008).
- Gonnelli, R. S. *et al.* Coexistence of two order parameters and a pseudogap in the iron-based superconductor $\text{LaFeAsO}_{1-x}\text{F}_x$. Preprint at <<http://arxiv.org/abs/0807.3149>>.
- Szabó, P. *et al.* Evidence for two-gap superconductivity and SDW pseudogap in $(\text{Ba}, \text{K})\text{Fe}_2\text{As}_2$ by directional point contact Andreev reflection spectroscopy. Preprint at <<http://arxiv.org/abs/0809.1566>>.
- Malone, L. *et al.* Magnetic penetration depth of single crystal $\text{SmFeAsO}_{1-x}\text{F}_x$: A fully gapped superconducting state. Preprint at <<http://arxiv.org/abs/0806.3908>>.
- Martin, C. *et al.* Nodeless superconducting gap in $\text{NdFeAsO}_{0.9}\text{F}_{0.1}$ single crystals from anisotropic penetration depth studies. Preprint at <<http://arxiv.org/abs/0807.0876>>.
- Ren, C. *et al.* Evidence for two gaps and breakdown of the Uemura plot in $\text{Ba}_{0.6}\text{K}_{0.4}\text{Fe}_2\text{As}_2$ single crystals. Preprint at <<http://arxiv.org/abs/0808.0805>>.
- Ding, H. *et al.* Observation of Fermi-surface-dependent nodeless superconducting gaps in $\text{Ba}_{0.6}\text{K}_{0.4}\text{Fe}_2\text{As}_2$. *Europhys. Lett.* **83**, 47001 (2008).
- Zhao, L. *et al.* Unusual superconducting gap in $(\text{Ba}, \text{K})\text{Fe}_2\text{As}_2$ superconductor. *Chin. Phys. Lett.* **25**, 4402–4405 (2008).
- Kondo, T. *et al.* Momentum dependence of the superconducting gap in $\text{NdFeAsO}_{0.9}\text{F}_{0.1}$ single crystals measured by angle resolved photoemission spectroscopy. *Phys. Rev. Lett.* **101**, 147003 (2008).
- Evtushinsky, D. V. *et al.* Momentum dependence of the superconducting gap in $\text{Ba}_{1-x}\text{K}_x\text{Fe}_2\text{As}_2$. Preprint at <<http://arxiv.org/abs/0809.4455>>.
- Mazin, I. I. *et al.* The challenge of unravelling magnetic properties in ferropnictides. *Phys. Rev. B* **78**, 085104 (2008).
- Yin, Z. P. *et al.* Electron-hole symmetry and magnetic coupling in antiferromagnetic LaOFeAs . *Phys. Rev. Lett.* **101**, 047001 (2008).
- Yildirim, T. Origin of the ~ 150 K anomaly in LaOFeAs ; competing antiferromagnetic superexchange interactions, frustration, and structural phase transition. *Phys. Rev. Lett.* **101**, 057010 (2008).
- Singh, D. J. & Du, M. H. Density functional study of $\text{LaFeAsO}_{1-x}\text{F}_x$: A low carrier density superconductor near itinerant magnetism. *Phys. Rev. Lett.* **100**, 237003 (2008).
- Haulé, K., Shim, J. H. & Kotliar, G. Correlated electronic structure of $\text{LaO}_{1-x}\text{F}_x\text{FeAs}$. *Phys. Rev. Lett.* **100**, 226402 (2008).
- de la Cruz, C. *et al.* Magnetic order close to superconductivity in the iron-based layered $\text{LaO}_{1-x}\text{F}_x\text{FeAs}$ systems. *Nature* **453**, 899–902 (2008).
- McGuire, M. A. *et al.* Phase transitions in LaFeAsO : structural, magnetic, elastic, and transport properties, heat capacity and Mössbauer spectra. *Phys. Rev. B* **78**, 094517 (2008).
- Koda, A. *et al.* *J. Phys. Condens. Matter* **17**, L257–L264 (2005).
- Rotter, M. *et al.* Superconductivity at 38 K in the iron arsenide $(\text{Ba}_{1-x}\text{K}_x)\text{Fe}_2\text{As}_2$. *Phys. Rev. Lett.* **101**, 107006 (2008).
- Klauss, H.-H. *et al.* Commensurate spin density wave in LaOFeAs : A local probe study. *Phys. Rev. Lett.* **101**, 077005 (2008).
- Chen, Y. *et al.* Magnetic order of the iron spins in NdOFeAs . *Phys. Rev. B* **78**, 064515 (2008).
- Qiu, Y. *et al.* Structure and magnetic order in the $\text{NdFeAs}(\text{O}, \text{F})$ superconductor system. Preprint at <<http://arxiv.org/abs/0806.2195>>.
- Zhao, J. *et al.* Structural and magnetic phase diagram of $\text{CeFeAsO}_{1-x}\text{F}_x$ and its relationship to high-temperature superconductivity. *Nature Mater.* **7**, 953–959 (2008).

25. Chen, G. F. *et al.* Superconductivity at 41 K and its competition with spin-density-wave instability in layered $\text{CeO}_{1-x}\text{F}_x\text{FeAs}$. *Phys. Rev. Lett.* **100**, 247002 (2008).
26. Huang, Q. *et al.* Magnetic order in BaFe_2As_2 , the parent compound of the FeAs based superconductors in a new structural family. Preprint at <<http://arxiv.org/abs/0806.2776>>.
27. Aczel, A. A. Muon spin relaxation studies of magnetic order and superfluid density in antiferromagnetic NdOFeAs , BaFe_2As_2 and superconducting $(\text{Ba}, \text{K})\text{Fe}_2\text{As}_2$. Preprint at <<http://arxiv.org/abs/0807.1044>>.
28. Wang, X. F. *et al.* Growth and anisotropy in transport properties and susceptibility of single crystals BaFe_2As_2 . Preprint at <<http://arxiv.org/abs/0806.2452>>.
29. Sefat, A. S. *et al.* Electronic correlations in the superconductor $\text{LaFeAsO}_{0.89}\text{F}_{0.11}$ with low carrier density. *Phys. Rev. B* **77**, 174503 (2008).
30. Pinsard-Gaudart, L., Berardan, D., Bobroff, J. & Dragoë, N. Large Seebeck coefficients in iron-oxypnictides: A new route towards *n*-type thermoelectric materials. *Phys. Status Solidi-Rapid Res. Lett.* **2**, 185–187 (2008).
31. Kreyssig, A. *et al.* Pressure-induced volume-collapsed tetragonal phase of CaFe_2As_2 as seen via neutron scattering. *Phys. Rev. B* **78**, 184517 (2008).
32. Park, T. *et al.* Pressure-induced superconductivity in single crystal CaFe_2As_2 . *J. Phys. Condens. Matter* **20**, 322204 (2008).
33. Alireza, P. *et al.* Superconductivity up to 29 K in SrFe_2As_2 and BaFe_2As_2 at high pressures. Preprint at <<http://arxiv.org/abs/0807.1896>>.
34. Pulikkoti, J. J., van Schilfgaarde, M. & Antropov, M. P. Competition between antiferromagnetic instability and frustrations in Fe–Se. Preprint at <<http://arxiv.org/abs/0809.0283>>.
35. Yildirim, T. The unprecedented giant coupling of Fe-spin state and the As–As hybridization in iron-pnictide. Preprint at <<http://arxiv.org/abs/0807.3936>>.
36. Fukuda, T. *et al.* Lattice dynamics of $\text{LaFeAsO}_{1-x}\text{F}_x$ and PrFeAsO_{1-y} via inelastic X-ray scattering and first-principles calculation. *J. Phys. Soc. Japan* **77**, 103715 (2008).
37. Zhao, J. *et al.* Spin and lattice structure of single crystal SrFe_2As_2 . *Phys. Rev. B* **78**, 140504 (2008).
38. Jesche, A. *et al.* Strong coupling between magnetic and structural order parameters in SrFe_2As_2 . *Phys. Rev. B* **78**, 180504 (2008).
39. Ishibashi, S., Terakura, K. & Hosono, H. A possible ground state and its electronic structure of a mother material (LaOFeAs) of new superconductors. *J. Phys. Soc. Japan* **77**, 053709 (2008).
40. Garcia, D. R. *et al.* Core level and valence band study of $\text{LaO}_{0.9}\text{F}_{0.1}\text{FeAs}$. Preprint at <<http://arxiv.org/abs/0810.3034>>.
41. Bondino, F. *et al.* Evidence for strong itinerant spin fluctuations in the normal state of $\text{CeFeAsO}(0.89)\text{F}(0.11)$ iron oxypnictides. *Phys. Rev. Lett.* (in the press).

Additional information

Reprints and permissions information is available online at <http://npg.nature.com/reprintsandpermissions>. Correspondence and requests for materials should be addressed to M.D.J.